

Moving average signals for the static compensator control

Abstract. The shunt static compensator with the control based on the average signals is presented. Two control signals are considered - moving RMS value of grid voltage and moving average power of the energy source. The compensator generates reactive current computed in the real time with the use of the iterative method. The multiport representation of the grid is presented. Analytical and simulation results show how the iterative control of the compensator behaves for three kinds of control signals.

Streszczenie. Opisano sterowanie kompensatora statycznego z wykorzystaniem dwóch rodzajów sygnałów – przesuwnej wartości skutecznej napięcia sieci i przesuwnej mocy czynnej źródła energii. Kompensator generuje prąd bierny obliczany w czasie rzeczywistym z wykorzystaniem metody iteracyjnej. Pokazano wielowrotkową reprezentację sieci elektrycznej. Analityczne i numeryczne wyniki pokazują jak przebiega sterowanie iteracyjne dla dwóch rodzajów sygnałów sterujących. **Zastosowanie kroczących sygnałów uśrednionych do sterowania kompensatora statycznego.**

Keywords: static compensator, moving average signals, iterative control, sliding mode, power flow.

Słowa kluczowe: kompensator statyczny, krocząca sygnały uśrednione, sterowanie iteracyjne, tryb ślizgowy przepływ mocy.

Introduction

A static compensator (STATCOM) is a member of the flexible alternating current transmission system (FACTS) devices [1], [2]. A STATCOM is installed in the electric networks with poor voltage regulation to improve these problems and improve stability of a network. Also voltage dips can be mitigated by using shunt-connected controlled current sources [3], [4]. Voltage dips are important failure influenced on power quality [5]. The improving of the power system flexibility is specially needed for the power system with a large share or renewable energy sources.

The STATCOM regulates voltage at its terminal by controlling the amount of reactive power injected into the power system. Such arrangements can be controlled by the local node voltage. The paper presents also the control based on average power signals measured at remote grid nodes.

For balanced three-phase systems d-q Park transformation enables to transform the system to the stationary frame [6]. Park transformation uses 3-phase sinusoidal functions. The product of these functions and 3-phase sinusoidal voltages or currents gives constant components and 2nd harmonic. 2nd harmonic is canceled as the result of three shifted sinusoids aggregation. The resulting instantaneous time functions are constant. Such process can be preceded by running techniques.

The stationary reference frame can be also achieved by averaging operation. The moving average operation transforms the instantaneous voltage, current and power into slowly changing signal. 2nd harmonic is eliminated as the result of the integration within the interval equal to the period. Exact period estimation is necessary condition to obtain the proper averaging [7]. The results obtained by the averaging operation is similar to the result of d-q transformation.

The control of the electronic inverter also can be achieved by two means. It can be done in feedback loop containing PI controller. The alternative solution can be achieved by applying iterative algorithms [8].

Compensators are installed in large electrical power systems and compensator location is essential for their effectiveness. Advanced methods are elaborated for choice the optimal place for compensators [9,10]. The paper presents port approach to analysis of electrical power systems. Port models of electrical grids seem to be more condensed than branch network models. Port models enable additional look at compensator control and location problems.

Multiport model of the power system

The considered compensator is oriented on the fundamental harmonic, higher harmonics are beyond the scope of this paper. Assuming that harmonic contents in the voltage is small the control can be based on the RMS value. The complex RMS values are denoted by capital letters U and I , vertical bars describe modules of these complex values $|U|$ and $|I|$. The control signal is achieved with the use of the iterative algorithm. Dominated approach to the power grid analysis is the network approach. A network includes such elements as branches, nodes and loops. Nodes represent buses in power system; branches represent transmission lines, transformers, consumers and generators. This paper presents the port approach to power grid analysis. The power grid is treated as a multiport.

The multiport shown in Fig. 1 contains k ports with compensators connected and n ports with independent voltage source connected.

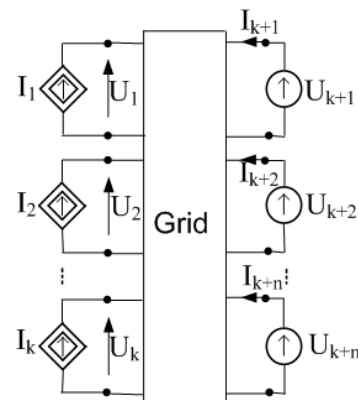


Fig.1. Multiport grid model

The compensators are modelled by controlled sinusoidal current sources. It is assumed that the grid comprised in the box does not contain independent sources, all sources are removed outside the box and connected to the port terminals. The circuit is linear and considered in the steady sinusoidal state. For such assumption the $(k+n)$ – port can be described by hybrid equation

$$(1) \quad \mathbf{Y} = \mathbf{HX}$$

where

$$(2) \quad \mathbf{X} = [I_1, I_2, \dots, I_k, U_{k+1}, U_{k+2}, \dots, U_{k+n}]^T$$

$$(3) \quad \mathbf{Y} = [U_1, U_2, \dots, U_k, I_{k+1}, I_{k+2}, \dots, I_{k+n}]^T$$

Elements h_{lj} of square matrix \mathbf{H} for $l=1, 2, \dots, k+n$ and $j=1, 2, \dots, k+n$ are complex numbers equal to open-circuit or short-circuit impedances or admittances

$$h_{lj} = \frac{Y_{lj}}{X_j} \text{ and } X_r = 0 \text{ for } r \neq j, j=1, 2, \dots, k+n$$

and $l=1, 2, \dots, k+n$.

There is no need to compute the multiport immitances during the iterative control. The iterative control is based on voltages $U_l (l=1, 2, 3, \dots, k)$ measured within the compensation process.

In the next section the detail investigation will be done for particular case of multiport $k=1, n=1$.

2-port with the static compensator connected

Assume that the compensator modelled by current source is connected to the 2-port as shown in Fig. 2.

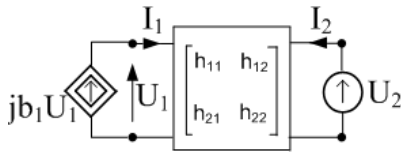


Fig. 2. 2-port with the independent voltage source and controlled current source

The circuit is linear and considered in the steady state. It means that the voltage source can be represented by complex RMS value U_2 and the circuit elements can be represented by their complex impedances and admittances.

The hybrid equations of the 2-port can be written as

$$(4) \quad U_1 = h_{11}I_1 + h_{12}U_2$$

$$(5) \quad I_2 = h_{21}I_1 + h_{22}U_2$$

The compensator modelled by current source is connected to the 2-port as shown in Fig. 2. It is assumed that the 2-port does not contain independent sources inside the box, so it is reciprocal. The current source $I_1 = j b_1 U_1$ is controlled by voltage U_1 of the port 1. The gain $j b_1$ is imaginary number. It means that current I_1 is shifted to voltage U_1 by $\pi/2$. Real coefficient b_1 is piece-wise constant and computed in the control process.

For the circuit in Fig. 3 equations (4) and (5) lead to the relation between two voltages

$$(6) \quad U_1 = \frac{h_{12}}{1 - j b_1 h_{11}} U_2$$

and current

$$(7) \quad I_2 = \left(\frac{-j b_1 h_{12} h_{21}}{1 - j b_1 h_{11}} + h_{22} \right) U_2$$

For the reciprocal 2-port $h_{21} = h_{12}$. Current component

$$\frac{-j b_1 h_{12} h_{21}}{1 - j b_1 h_{11}} U_2$$

flowing in source U_2 is caused by the compensator, as it is equal to zero for $b_1 = 0$. The additional average power drawn from source U_2 can be expressed as

$$(8) \quad P_2 = \text{real} \left(\frac{-j b_1 h_{12} h_{21}}{1 - j b_1 h_{11}} |U_2|^2 \right)$$

Average power (7) depends on control parameter b_1 .

The influence of the compensator on the average power drawn from the energy source is illustrated in the next section.

The simulation presented in this section shows how the compensator can be controlled. Three control signals are presented: voltage $|U_1|$, power P_2 and root of power $\sqrt{P_2}$.

Each of these quantities depends on compensator gain b_1 . These dependents are seen in (6) and (8).

The iterative control of the compensator is described in [5]. For each chosen control signal the method is formulated as the optimization problem.

For control signal $|U_1|$:

Find compensator parameter b_1 such that grid voltage $|U_1|$ at the compensator port is close to desirable value U_d .

The iterative algorithm based on the secant method can be comprised in the following steps.

Step 0. Measure voltage $|U_0|$ for zero compensator current

$$(9) \quad b_0 = 0$$

Step 1. Measure voltage $|U_1|$ for optional chosen nonzero compensator parameter b_1 such that $|I_1| = |b_1| |U_0| < I_{\max}$.

Step k. Measure voltage $|U_k|$ and compute parameters b_k

$$(10) \quad b_k = \frac{|U_0| - U_d}{|U_0| - |U_{k-1}|} b_{k-1}$$

for $k=2, \dots, K$, where final index K is such that condition $(||U_K| - U_d|) < U_{\min}$ is fulfilled.

The algorithm given in equation (10) can be replaced by modified algorithm adequate for PWM inverter control [8]. Voltage $|U_k|$ can be replaced for other control signals. The algorithm (10) looks similarly. Quantities in (10) should be substituted as follows: $|U_1|$ and U_d should be changed for P_2 or $\sqrt{P_2}$ and P_d or $\sqrt{P_d}$.

Simulation results for 2-port circuit

Presented simulation was obtained with the use of PLECS program.

The PLECS block model of the single phase grid with compensator represented by controlled current source I is shown in Fig. 3.

The PLECS model presented in Fig. 3 contains two subsystems – *State Machine* and *Subsystem*. *State machine* is shown in Fig. 4, *Subsystem* shown in Fig. 5 represents electrical circuit of the grid.

State machine shown in Fig. 4 executes the algorithm presented in equations (9), (10). The algorithm seen in *State Machine* uses as control signal average power P drawn from independent voltage source V_{ac} (Fig. 5) instead of the voltage RMS $|U|$

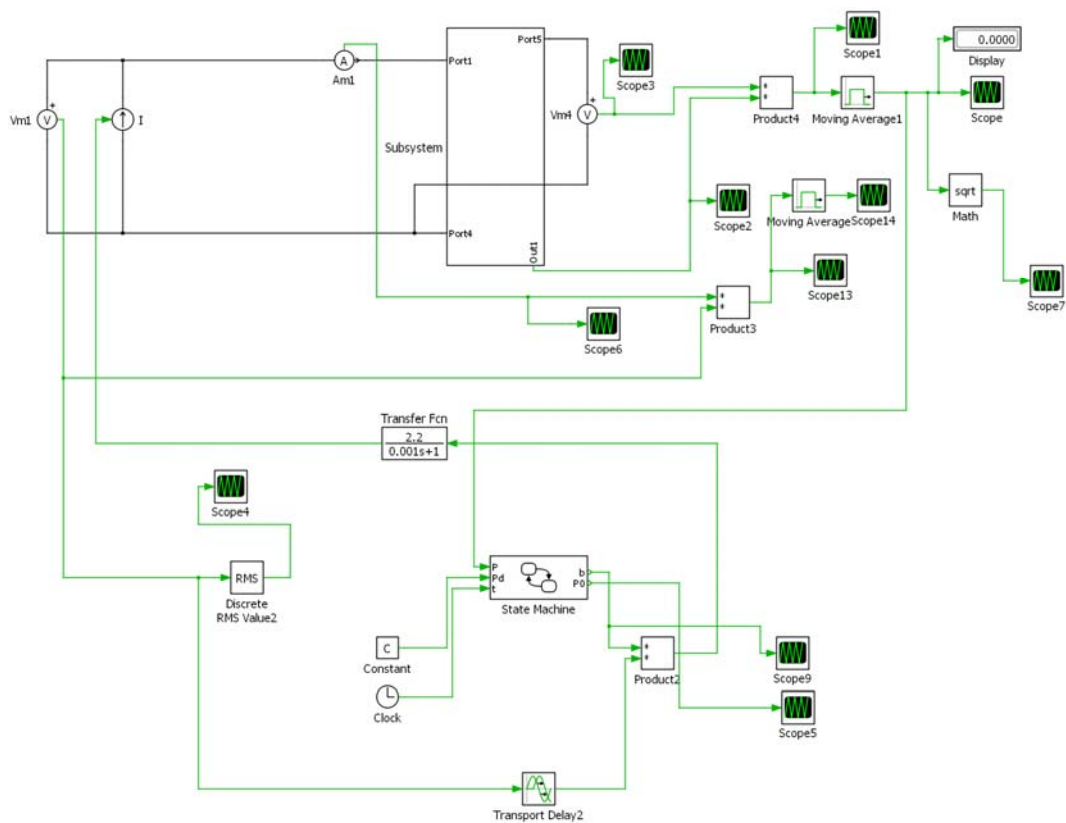


Fig. 3. PLECS model of the grid and compensator with the iterative control

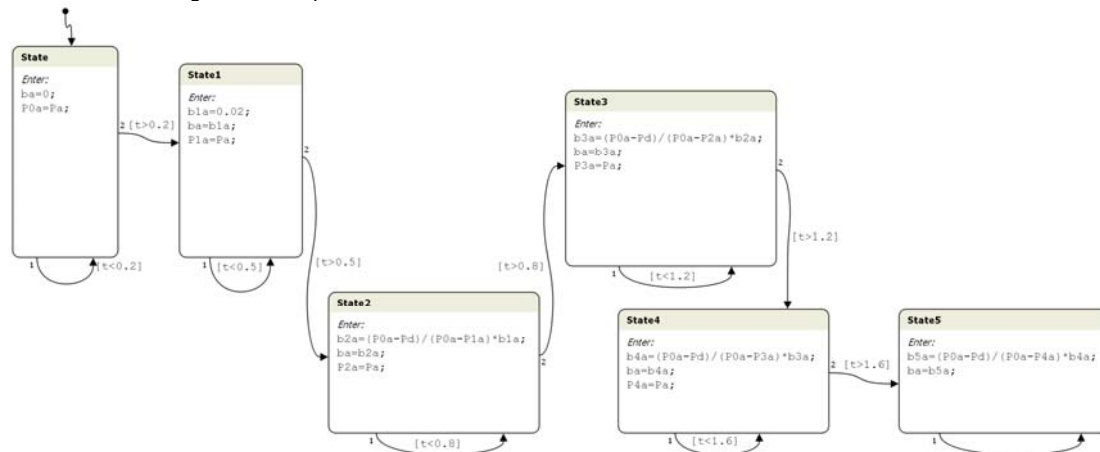


Fig. 4. State machine

State machine contains 6 state boxes. Each state responds to one algorithm step. Transitions are represented by curved arrows from one state to another. The time intervals are defined by the condition trigger written for each transition.

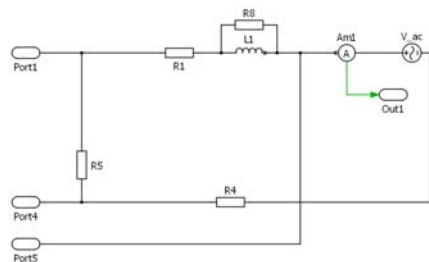


Fig.5. Grid model (Subsystem)

Electrical subsystem embedded to PLECS model (Fig. 3) is shown in Fig. 5. Port1 and Port2 seen in Fig.5 create the input port of the general 2-port given in Fig. 2. Port4

and Port5 connected to the source nodes create the output port of the 2-port.

Parameters of the grid model were assumed as follows

$$R_1 = 0.3\Omega, R_4 = 0, R_5 = 100\Omega, R_8 = 1000\Omega, \text{ Voltage source } L_1 = 0.004H$$

amplitude $V_{ac} = 300V$, frequency $f = 50Hz$.

PLECS model shown in Fig. 3 is universal, because it contains 3 different signals available – grid voltage at the compensator nodes (Scope4), average power drawn from source voltage (Scope) and square root of the average power (Scope7). The simulations presented below make use of the individual signal.

Figs. 6 to 10 show the simulation results. Time (seconds) is shown on x-axis, on y-axis voltage is given in volts, power in wats.

Comparing the waveforms shown in Fig. 9 and Fig. 11 we can see, that root of power as the control signal leads to smaller oscillation within the iterative process. However, root operation needs considerable computational outlays.

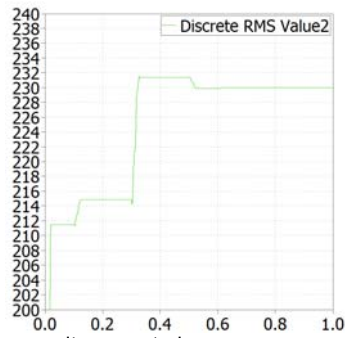


Fig. 6. RMS voltage - voltage control

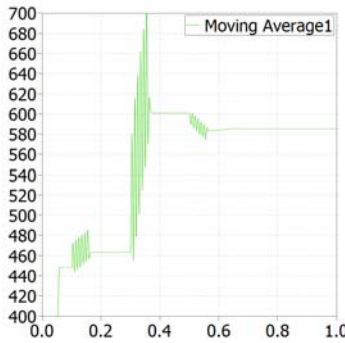


Fig. 7. Average power - voltage control

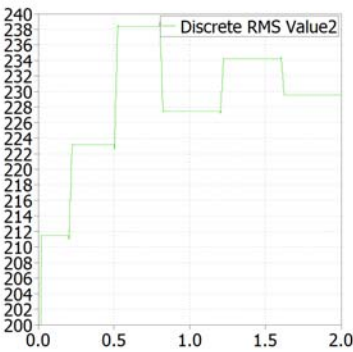


Fig. 8. RMS voltage – power control

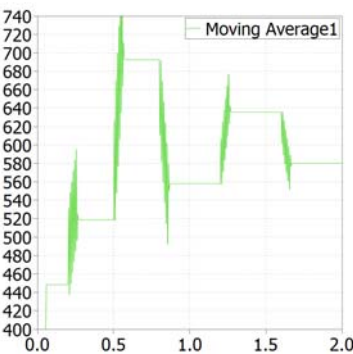


Fig. 9. Moving average power – power control

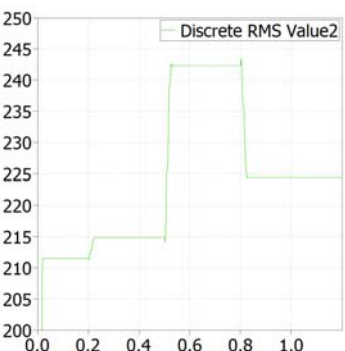


Fig. 10. RMS voltage – root of power control

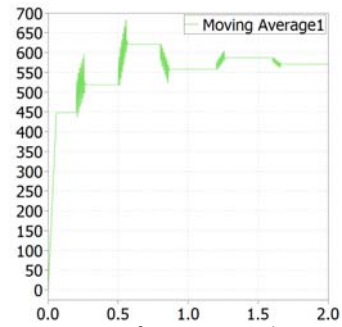


Fig. 11. Average power – root of power control

The process of the iterative control can provide additional information about the electrical power system. For example, from equations (4) and (5) we can see that system parameters can be estimated as

$$|h_{12}| = \frac{|U_{10}|}{|U_2|}, |h_{11}| = \frac{|U_{1c}|}{|I_{1c}| |U_{10}|}$$

where index 0 means the state without compensator and index c means the compensator current equal to I_{1c} .

3-port system analysis

Further analysis is narrowed to the system with two independent voltage sources and one compensator, as shown in Fig. 12.

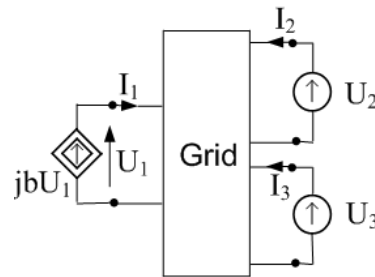


Fig.12. System with two independent sources

3-port in Fig.12 is the particular case of the multiport shown in Fig. 11 for $k = 1$ and $n = 2$.

The hybrid equations for this 3-port are as follows

$$(10) \quad U_1 = h_{11}I_1 + h_{12}U_2 + h_{13}U_3$$

$$(11) \quad I_2 = h_{21}I_1 + h_{22}U_2 + h_{23}U_3$$

$$(12) \quad I_3 = h_{31}I_1 + h_{32}U_2 + h_{33}U_3$$

and

$$(13) \quad I_1 = jb_1U_1$$

From (10) and (13)

$$(14) \quad U_1 = \frac{h_{12}U_2 + h_{13}U_3}{1 - jb_1h_{11}}$$

Eliminating compensator current I_1 from (14) and (15) the system of three equations is reduced to two equations with two independent voltages U_2, U_3 and compensator gain b_1

$$(15) \quad I_2 = Y_{22}U_2 + Y_{23}U_3$$

$$(16) \quad I_3 = Y_{32}U_2 + Y_{33}U_3$$

where

$$(17) \quad Y_{22} = \frac{jb_1h_{21}^2}{1 - jb_1h_{11}} + h_{22}$$

$$(18) \quad Y_{23} = \frac{jb_1h_{21}h_{13}}{1 - jb_1h_{11}} + h_{23}$$

$$(19) \quad Y_{32} = \frac{jb_1 h_{31} h_{12}}{1 - jb_1 h_{11}} + h_{32}$$

$$(20) \quad Y_{33} = \frac{jb_1 h_{31}^2}{1 - jb_1 h_{11}} + h_{33}$$

Average power drawn from the voltage sources is

$$(21) \quad P_2 = \text{real}(U_2^* I_2)$$

$$(22) \quad P_3 = \text{real}(U_3^* I_3)$$

The stars denote conjugate complex number.

Detail investigation will be done for the particular case of the 3-port shown in Fig. 13.

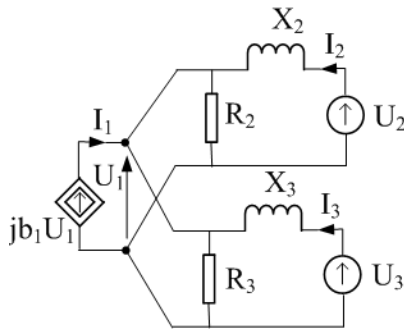


Fig. 13. 3-port with RL components

The circuit in Fig. 13 is composed of passive linear elements replaced by two series connected reactances $X_2 = \omega L_2$, $X_3 = \omega L_3$ and two shunt resistances R_2 , R_3 . This impedances form the 3-port. The hybrid parameters of this 3-port can be obtained using procedure given below equation (3).

$$h_{11} = \frac{1}{G_2 + G_3 - j(B_2 + B_3)},$$

$$h_{12} = \frac{-jB_2}{G_2 + G_3 - j(B_2 + B_3)},$$

$$h_{13} = \frac{-jB_3}{G_2 + G_3 - j(B_2 + B_3)},$$

$$h_{21} = -h_{12},$$

$$h_{22} = \frac{1}{jX_2 + \frac{1}{G_2 + G_3 - jB_3}},$$

$$h_{23} = \frac{B_2 B_3}{G_2 + G_3 - j(B_2 + B_3)},$$

$$h_{31} = -h_{13},$$

$$h_{32} = h_{23},$$

$$h_{33} = \frac{1}{jX_3 + \frac{1}{G_2 + G_3 - jB_2}}.$$

For convenience, denotations $G = 1/R$, $B = 1/X$ are used, with $X = \omega L$ or $X = -1/\omega C$.

Let the source voltages be given in the following form

$$(23) \quad U_2 = r_2 U_g e^{j\delta_2}$$

$$(24) \quad U_3 = r_3 U_g e^{j\delta_3}$$

where U_g , r_2 , r_3 , δ_2 , δ_3 are real numbers.

The source powers according to (21), (22) and (15), (16) can be written as

$$(25) \quad P_2 = U_g^2 \text{real}(r_2^2 Y_{22} + r_2 r_3 e^{j(\delta_3 - \delta_2)} Y_{23})$$

$$(26) \quad P_3 = U_g^2 \text{real}(r_3^2 Y_{33} + r_2 r_3 e^{j(\delta_2 - \delta_3)} Y_{32})$$

In order to observe the influence of the compensator current $b_1 U_1$ on the average power flow between two voltage sources, the non-dissipative circuit will be considered. Let the system parameters be taken as follows $G_2 = 0$, $G_3 = 0$. Additionally let $B_2 = B_3 = B$ and $r_2 = 1$, $\delta_2 = 0$. For such assumptions, using the given above expressions for hybrid coefficients and equations (17) - (20), the power can be expressed in the simple analytical form

$$(27) \quad P_2 = \frac{1}{2} r_3 B U_g^2 \left(\frac{\frac{b_1}{B}}{2 + \frac{b_1}{B}} - 1 \right) \sin \delta_3$$

and

$$(28) \quad P_3 = -P_2$$

Relation (28) is obvious as the considered 3-port does not contain resistors. The average power is exchanged between sources U_1 and U_2 . The voltage at the compensator port can be expressed as

$$(29) \quad U_1 = \frac{(1 + r_3 e^{j\delta_3}) U_g}{2 + \frac{b_1}{B}}$$

Equation (27) can be written as

$$(30) \quad P_2 = c_1 r_3 P_s \sin \delta_3$$

where compensator coefficient c_1

$$(31) \quad c_1 = \frac{1}{2} \left(\frac{\beta_1}{2 + \beta_1} - 1 \right)$$

relative compensator gain

$$(32) \quad \beta_1 = \frac{b_1}{B}$$

and rating power

$$(33) \quad P_s = B U_g^2$$

The power flow can be controlled with the aid of two source parameters δ_3 , r_3 and one compensator parameter β_1 . Fig.14 shows function $c_1 = f(\beta_1)$ for two intervals of β_1 . The system admittance B can be positive or negative. Positive for inductive character of the system seen from port '1', negative for capacitive character. Compensator gain b_1 also can be positive or negative.

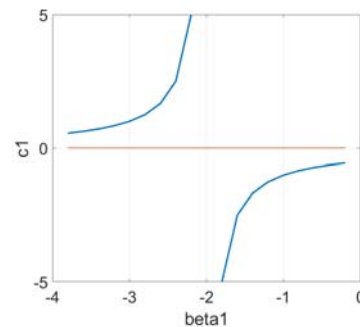


Fig. 14. Relation between compensator gain β_1 and compensator coefficient c_1

Function $c_1 = f(\beta_1)$ has singular point at $\beta_1 = 2$. Such location of the singularity is the consequence of circuit parameters $B_2 = B_3$. At this singular point coefficient c_1 changes its sign from positive to negative. It means that the power flow between sources changes its direction. Such situation can be observed in the non dissipative circuit for big compensator current.

When compensators are used the block of system control can be sketched as shown on Fig. 15.

Two sets of the input signals δ and r are associated with the chosen set of independent sources, set of signals b contains the compensator gains. The set of output signals U contains RMS values of the voltages at the compensator

Numerical example

ports. The set of output signals P contains average power of the chosen system sources.

The PLECS model shown in Fig. 16 has the structure of the 3-port shown in Fig. 12.

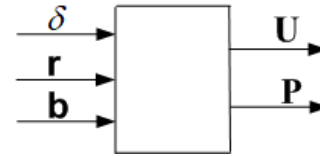


Fig.15. Block of system control

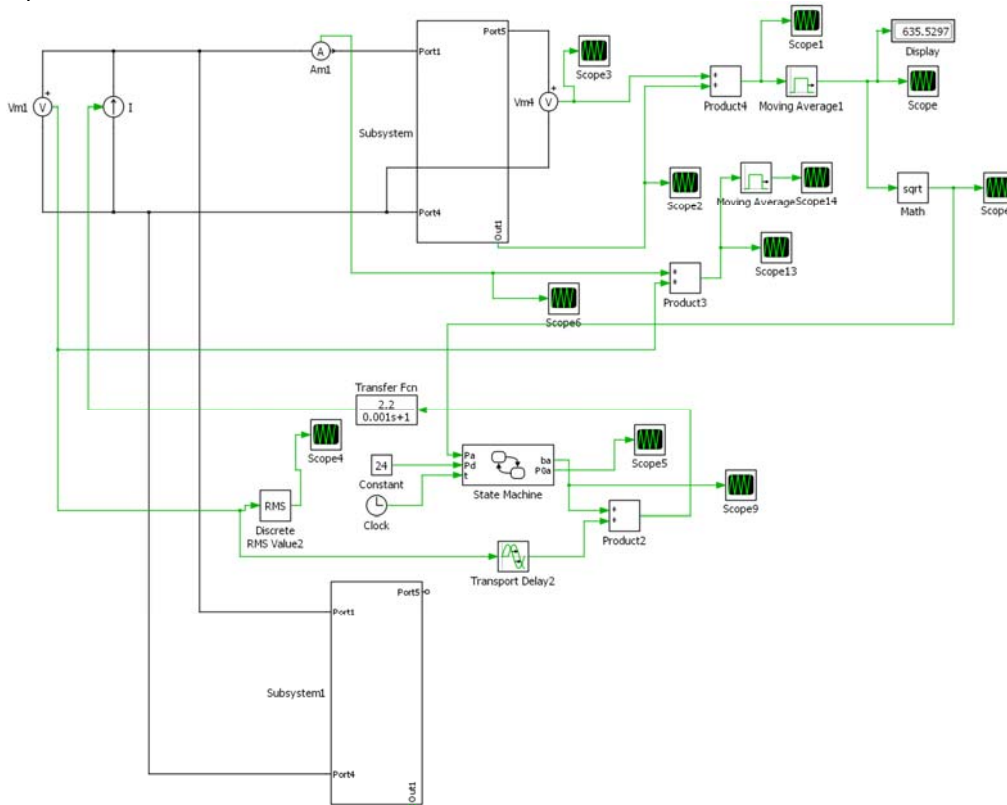


Fig. 16. PLECS model of the two grids and one compensator with the iterative control

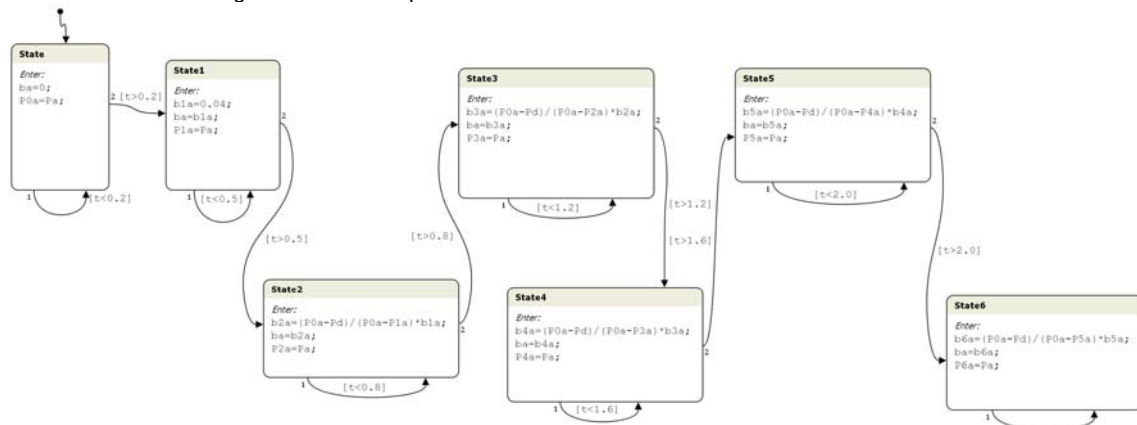


Fig. 18. State machine

The grid is composed of two circuits. The first of these two circuits contained in *Subsystem* is shown in Fig. 17. The parameters of this circuit are chosen as follows $R_1 = 0.3\Omega$, $R_4 = 0$, $R_5 = 100\Omega$, $R_8 = 1000\Omega$, $L_1 = 0.004H$, $V_{ac} = 300V$, $f = 50Hz$, $phase = 0$.

The second part of the grid is contained in *Subsystem 1*. The structure of *Subsystem1* is the same as given in Fig. 17. Parameters remain the same except for $R_5 = 200\Omega$.

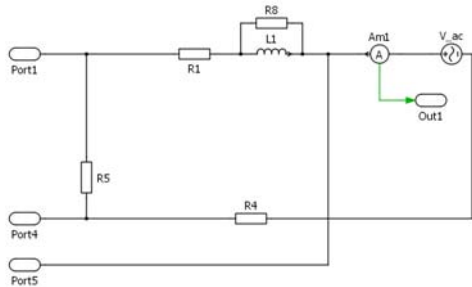


Fig. 17. One part of the grid

The controlled current source seen in Fig. 16 plays the role of compensator. The control signal for this current source is worked out in the system contained *State Machine* shown in Fig. 18.

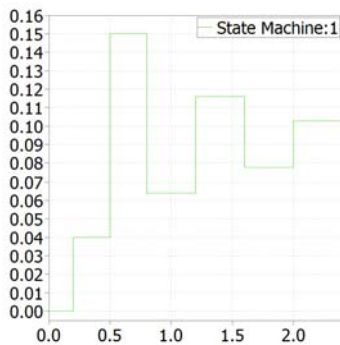


Fig. 19. Gain of the controlled current source

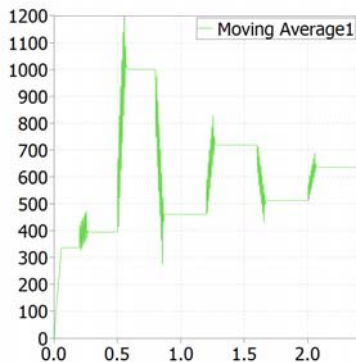


Fig. 20. Power drawn from the independent voltage source V_{ac} seen in Fig. 17

The state machine shown in Fig. 18 realizes six steps of the iterative algorithm. The root of power drawn from the independent voltage source of the first grid plays the role of the control signal. Demanded value of this signal is chosen equal to 24, as it is seen in Fig.17. It means that demanded source power is 576 W.

Simulation results are shown in Fig. 19 and 20. The iterative process is seen Fig. 19. Initial gain b of the current source is chosen equal to 0.04. In the sixth step the gain rises to 0.1. As the result the average power drawn from the source V_{ac} placed in the first grid reaches 635 W.

Conclusions

The analytical and numerical results presented in the paper were obtained for the circuit models of the electrical grid. Generators are modeled by the independent voltage sources. Consumers and lines are substituted by RLC circuit elements. Such approximation is far from real power system. In real systems electrical motors dominate among

energy consumers. Modeling such consumers by RL elements is very rough. However, the circuits used in the paper make possible to observe the nature of the real system.

Presented in the paper multiport model of an electrical grid contains k compensator ports and n source ports. As the multiport is reciprocal it does not contain sources inside the box. In real grids numbers of independent voltage sources representing generators is large, but not all sources should be observed. Though, in Fig. 1 and in equation (1) number n should be equal to the number of all independent sources, as the multiport is reciprocal it does not contain sources inside the box. But only those sources should be observed whose currents are used for the compensator control. Some of k compensators can be replaced by open circuits. The voltages of such ports can be observed and used for control of other compensators. Multiport representation of the grid, as shown in Fig. 1, concerns sinusoidal steady state and complex numbers h are sufficient for the system analysis in this state. But these numbers are not exploited while compensator control.

The used circuit models are not need for the iterative compensator control. From the analysis of the n -ports containing independent voltage sources and controlled current sources can be issued conclusions, that compensators can be treated as the additional aid for the control of average power flow between sources and consumers. Compensators can stabilize voltage at chosen ports and influence on power derived from sources.

Authors: dr inż. Jacek Korytkowski, prof. dr hab. inż. Kazimierz Mikołajuk, dr hab. inż. Krzysztof Siwek, mgr inż. Andrzej Toboła, Politechnika Warszawska, Instytut Elektrotechniki Teoretycznej i Systemów Informacyjno-Pomiarowych, ul. Koszykowa 75, 00-661 Warszawa, E-mail: Jacek.Korytkowski@pw.edu.pl, Kazimierz.Mikolajuk@ee.pw.edu.pl, Krzysztof.Siwiek@ee.pw.edu.pl, Andrzej.Tobola@ee.pw.edu.pl

REFERENCES

- [1] F. Shahnia, S. Rajakaruna, A. Ghosh Static Compensators (STATCOMs) in Power Systems; Springer, 2015.
- [2] N. G. Higorani, L. Gyugyi, Understanding FACTS – Concepts and Technology of Flexible AC Transmission System. IEEE Press, New York, 2000.
- [3] M. Bongiorno, J. Svensson, Voltage Dip Mitigation Using Shunt-connected Voltage Source Converter. IEEE Trans Power Electron 22(5), 2007.
- [4] J. Milanovic, Y. Zhang, Modeling of FCTS Devices for Voltage Sag Mitigation Studies in Large Power Systems. IEEE Trans. Power Delivery Vol. 25, (4), 2010, pp. 3044-3052.
- [5] A. Baggini, Z. Hanzelka, Firlit, A.; S. Moskwa, T. Rodziewicz, Handbook of Power Reliability. AGH Kraków, Poland, 2021.
- [6] J. M. Maza-Ortega, J. Rosendo-Macias, A. Gomez-Exposito, S. Celballos-Mannozi, M. Barragan-Villarejo, Reference Current Computation for Active Power Filters by Running DFT Techniques. IEEE Transactions Power Delivery, Vol. 25, (3), 2010, pp. 1986-1995.
- [7] K. Mikołajuk, Z. Staroszczyk, A. Toboła, Synchronization of the Iterative Process for Voltage Harmonic Mitigation. Przegląd Elektrotechniczny 6/2019, pp. 97-104.
- [8] K. Mikołajuk, K. Siwek, A. Toboła, Iterative Control of the Static Compensator. Przegląd Elektrotechniczny 5/2021, 2021, pp.134-139.
- [9] E. N. Azadani, S.H. Hosseinian, M. Janati, P. Hasanpor, Optimal Placement of Multiple STATCOM, 12th International Middle-East Power System Conference, 2008, pp. 523-528.
- [10] C. A. Ferreira, V. M. da Costa, A Second Order Power Flow Based on Current Injection Equations. Int. J. Electric Power Energy Syst. 15(2), 2005, 508-514.
- [11] S. Song, C. Han, G. Lee, R. A. McCann, G. Jang, Voltage Sensitivity Approach-Based Adaptive Droop Control Strategy of Hybrid STATCOM. IEEE Trans. on Power Systems, No. 1, 2021, pp. 389-401.